New Analysis Methods for Comprehensive Understanding of Random Telegraph Noise

T. Nagumo, K. Takeuchi, S. Yokogawa*, K. Imai* and Y. Hayashi
LSI Fundamental Research Lab. / Advanced Device Development Division*, NEC Electronics Corporation
1120 Shimokuzawa, Sagamihara, Kanagawa 229-1198, Japan
+81-42-771-0690, Fax +81-42-771-0692, toshiharu.nagumo@necel.com

Abstract

New analysis methods useful for understanding both complex waveforms and statistical behaviors of Random Telegraph Noise (RTN) are proposed. Complex waveforms are clearly visualized using Time Lag Plots. Bias dependence of statistically extracted average trap number is discussed, with emphasis on the importance of undetectable traps on product reliability.

1. Introduction

It is predicted that, as transistors are scaled, RTN will emerge as a serious reliability issue for SRAM operations [1-3]. Since RTN is a statistical phenomenon, to fully understand its impact on circuits, it is necessary to assess the probability distributions of trap numbers, amplitude, and capture/emission time (τc/τe), as well as their dependence on bias and temperature. However, there are various factors that make this task difficult; 1) Many samples must be measured to obtain statistical information; 2) Some traps are so slow (e.g. τ~1hour) [4] that very long time measurement is necessary; 3) Some traps are so fast that their detection is limited by the sampling speed; 4) Waveforms are often very complex (examples are in Fig. 4). In a previous work [3], issues 1) and 2) were addressed by combining addressable device matrix array (DMA) and virtual parallel measurement. In this work, issues 1), 3) and 4) will be addressed. Fast source-measure units (SMUs) capable of 1Msps sampling are used (Fig. 1). Standard 4 pad devices are used instead of DMA's, since DMA's are not suited for fast measurement due to their high on-chip parasitic resistance. A visualization tool for complex waveforms, a methodology for extracting basic parameters from fewer numbers of samples than DMA's, and extracted gate bias dependence of average trap number will be presented. Limitation of detectable range of RTN is also discussed.

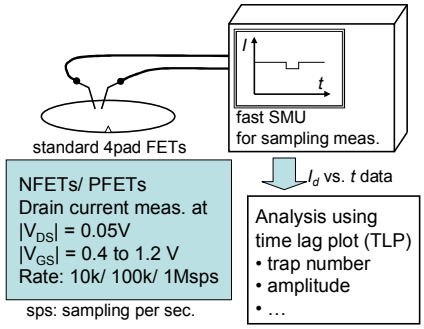

Fig. 1 Overview of measurement condition and analysis of this work.

2. Time Lag Plot

Complexity of RTN waveforms is a major obstacle for understanding RTN behavior. To overcome this issue, use of a Time Lag Plot (TLP) is proposed (Figs. 2 and 3). TLP can be drawn by simply plotting points in an *x*-*y* plane, where *x* is set to *i*-th sampled data, and *y* to the next (*i*+1)-th sampled data. TLPs make it possible to easily count the number of multiple traps. Even existence of traps faster than the SMU sampling rate can be recognized using TLP. These features will be explained showing several examples.

Fig.4(a) shows the first example (sample B). TLP clearly shows that at least four states 00, 01, 10 and 11 (i.e. two traps) exist. Though this can be also recognized from the time domain waveform, it is less easy. Results for another sample C are shown in Figs.4(b) and 4(c). In Fig.4(b), the waveform spikes downward with irregular amplitudes, the cause of which is not apparent at first sight. TLP reveals the reason; there are four states, two of which 10 and 11 are too fast to be captured by the 10ksps sampling. By increasing the sampling speed to 100ksps, the four states are fully resolved by TLP, as shown in Fig.4(c). Another example (sample D) is shown in Figs.4(d) to 4(f). TLP at 10ksps suggests that four states exist, two of which 10 and 01 are overlapped (Fig.4(d)). In this case, the TLP spots are highly smeared due to some additional noise. Increased sampling rate combined with TLP reveals that this additional noise is actually RTN, switching between states 0xx and 1xx, where the duration of stay at 1xx is very short, as shown in Figs.4(e). By increasing the sampling rate to 1Msps, the short duration state 100 is clearly resolved by TLP (Fig.4(f)). It is noticed that the TLP shape, which is usually square, is skewed in Fig.4(f). This is because of the CR delay (~2μs) of the measurement system. CR time constant can be easily assessed from the slope of the skew, as shown in Fig.4(f). Fourier transform of the data in the smeared spot is also effective. Fig. 5 shows a power spectral density for a TLP spot in Fig. 4(a), state 11. Lorenzian spectrum suggests existence of RTN.

From the results in Fig.4, it can be concluded that complex waveforms are caused by both insufficient time resolution of the measurement systems and existence of multiple traps. TLP is a useful tool for the interpretation of complex waveforms.

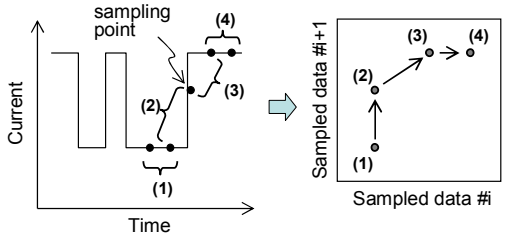

Fig. 2 Explanation of Time Lag Plot (TLP). TLP visualizes autocorrelation of waveforms.

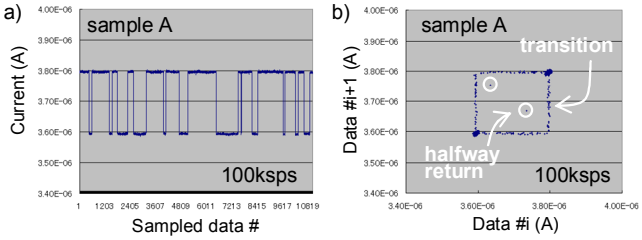

Fig. 3 a) waveform and b) Time Lag Plot (TLP) for simple two state RTN.

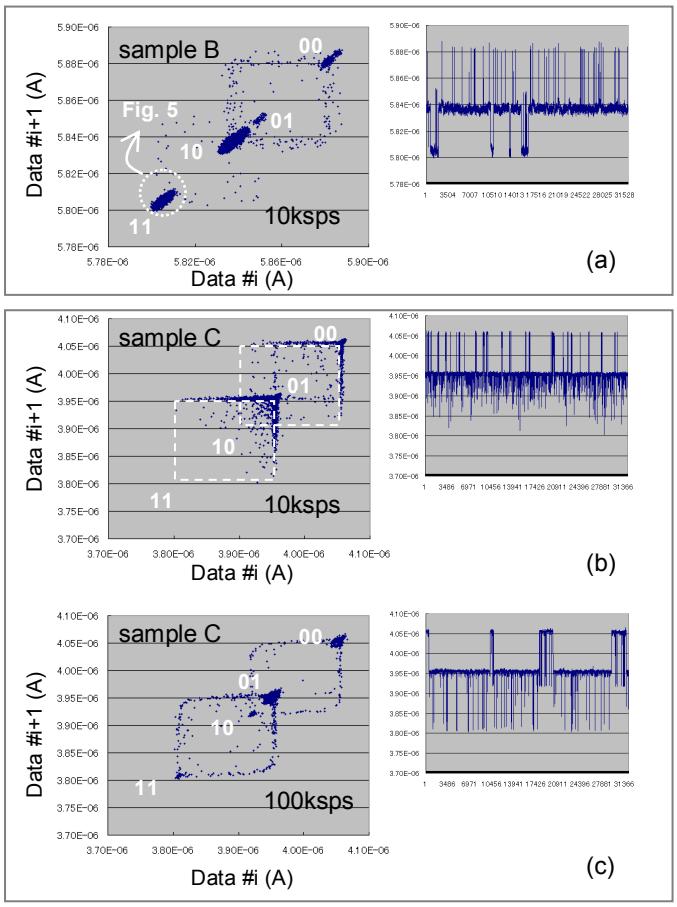

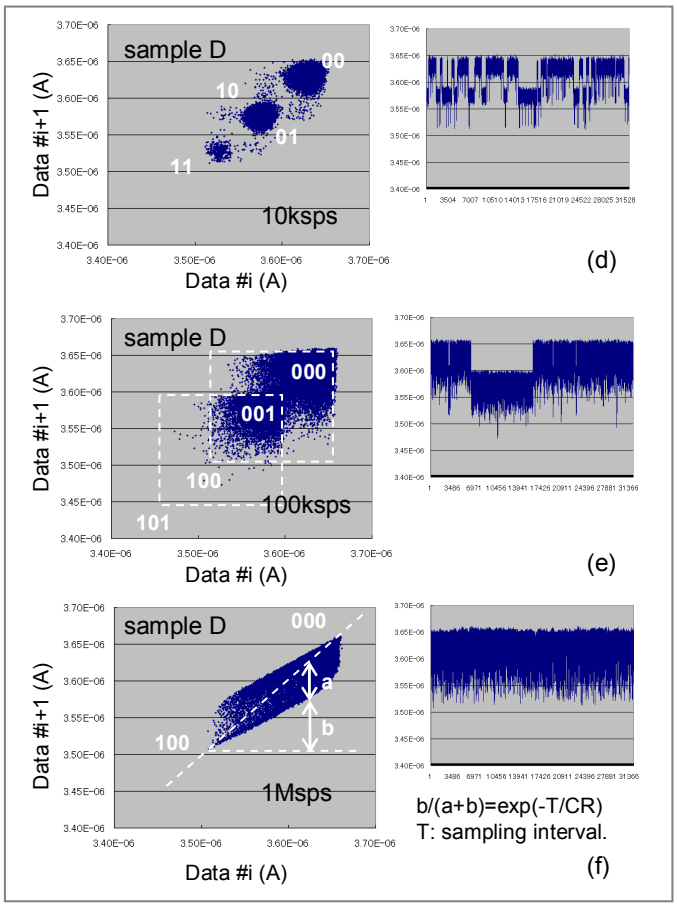

Fig. 4 Examples of Time Lag Plots (TLPs) and corresponding waveforms. (a) sample B, (b)-(c) sample C, (d)-(f) sample D.

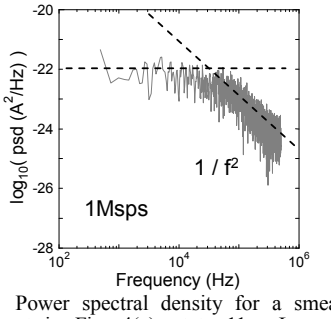

Fig.5 Power spectral density for a smeared TLP spot in Fig. 4(a), state 11. Lorenzian spectrum suggests existence of RTN.

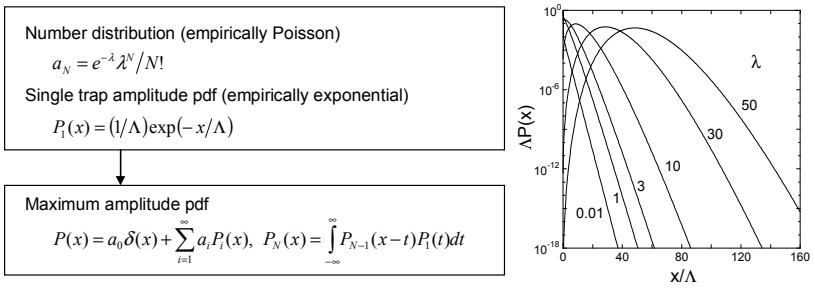

Fig. 6 Maximum amplitude model [3].

3. Statistical Parameter Extraction

According to a model proposed in [3], probability density functions of RTN amplitude can be calculated if average trap number λ and average single trap amplitude Λ are known (Fig.6). With the aid of TLPs, λ and Λ were extracted without using DMA's (i.e. using a fewer number of devices). First, by using a semi-automated program, the numbers of traps in each device were extracted. The number of discrete current levels is counted from the measured waveforms, and then it is translated into the number of traps. If $2^{(n-1)} <$ (current levels) $\leq 2^n$, then the trap number is regarded as n. In the counting procedure, only data points in the vicinity of $y=x$ line in a TLP are used (Fig.7). This enhances accuracy of extraction, since imperfectly sampled data are discarded. After n in all measured devices are counted, λ is extracted. In [3], Λ was directly extracted from the selected devices having only one trap per device. However, this is not possible when the number of available devices is limited. Therefore, instead, Λ was determined by fitting, as shown in Fig.8. Once λ is known, theoretical probability distribution of maximum amplitude normalized by Λ can be calculated (Fig. 6). Then, the theoretical distribution is fitted with measured peak-to-peak amplitude distributions by adjusting Λ.

By using the above method, statistical parameters of RTN can be evaluated using standard 4 pad devices. NFETs and PFETs with gate length of 54 nm and gate width of 126 nm are evaluated. Examples of number distributions and extracted gate voltage dependence of λ are shown in Figs. 9 and 10, respectively. Strong dependence of λ on V_{GS} is demonstrated, while that on substrate concentration N_{ch} is insignificant. It is often reported that RTN is more serious in PFETs than NFETs [1][5]. However, this relationship may be reversed, if V_{GS} is small. Fig. 11 shows extracted Λ for $\Delta I_D/I_D$ vs V_{GS}. Λ decreases as V_{GS} increases, in agreement with TCAD predictions [6].

4. Detectable Range

It should be noted that λ in Fig. 10 is not the number of *existing* traps, which should be constant, but that of *detectable* traps. Fig.12 shows V_{GS} dependence of τe and τc for some of the individual RTN signals. Two types of traps

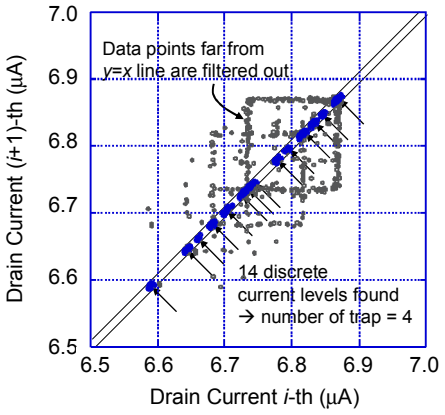

Fig. 7 Filtering of data points using TLP and extraction of number of states. Number of discrete current levels are counted using the data points near $y=x$ line and then it is translated into number of traps.

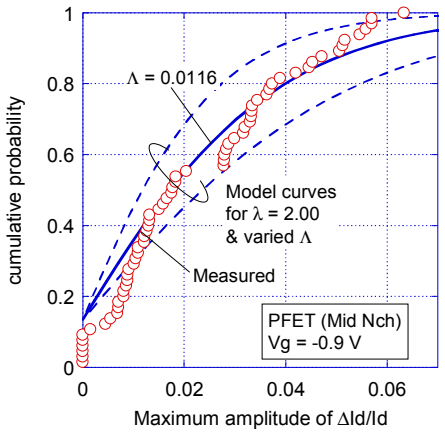

Fig. 8 Extraction of average single trap amplitude Λ. Calculated probability distributions of maximum amplitude using extracted average trap number λ is fitted to measured distributions by adjusting Λ. In this case Λ is extracted as 0.0116.

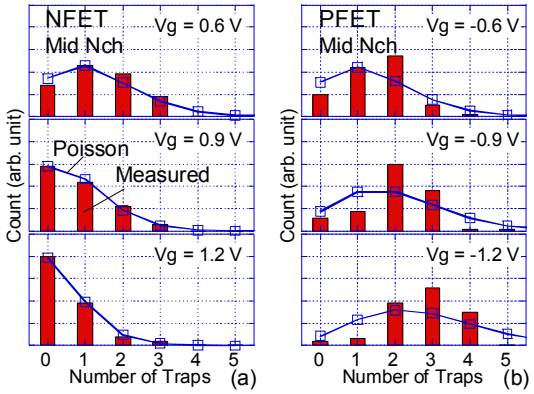

Fig. 9 Histograms of detected number of traps in the same transistor for three different gate bias conditions. (a) NFET and (b) PFET.

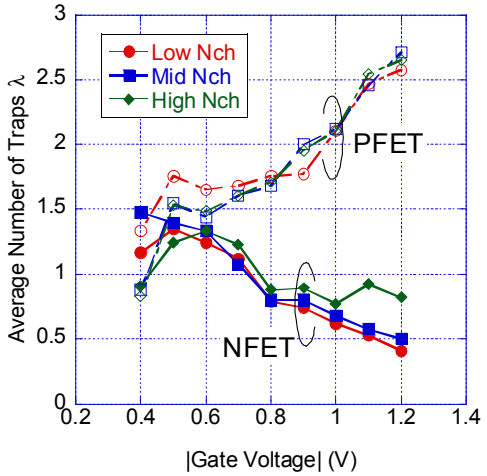

Fig. 10 Gate voltage dependence of average number of traps λ. V_{GS}, dependence of λ show opposite trends in NFETs and PFETs.

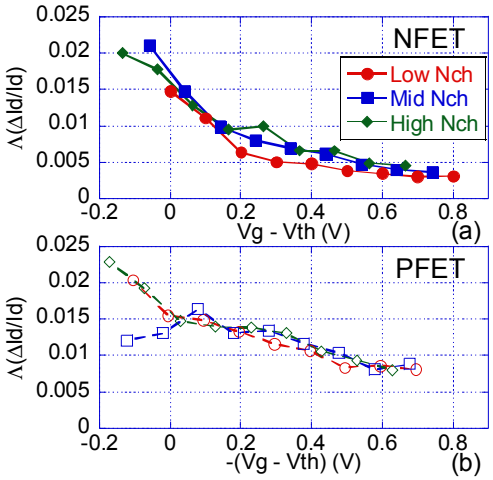

Fig. 11 Extracted gate voltage dependence of Λ for $\Delta I_d/I_d$. (a) NFET and (b) PFET. $\Delta I_d/I_d$ amplitude by single trap decreases with increasing V_{GS}

exhibiting different V_{GS} dependence exist: presumably one-way type and round-trip type. Traps A and D are regarded as one-way type, and B, C, and E as round-trip type. In either case, due to limited measurement duration and sampling speed, only traps having both τe and τc within a certain time range can be detected.

Due to the dependence of τe and τc on V_{GS}, whether a specific trap is detectable or not depends on V_{GS}, as shown in Fig. 13(a). A round-trip type trap is discussed here as an example. Even if a trap is detected at a certain condition (e.g. $V_{GS} = V_{G1}$), the trap can no longer be detected at a different condition in the shaded V_{GS} range, where either τe or τc is out of detectable range (e.g. $V_{GS} = V_{G2}$). The detectable V_{GS} range is related with the alignment of the trap energy level E_T and the Fermi level E_F [7]. If E_T and E_F are aligned within a few kT (Fig. 13(b)), it is more likely that the trap is detectable, because τe and τc are close to each other. However, if E_T and E_F are apart (Fig. 13(c)), since capture or emission rarely occurs, detection of the trap is difficult.

Undetectable traps may affect reliability of products, whose lifetime is much longer, and circuit operation much faster than the measurement. Estimation of the effects of undetectable traps will be a major challenge for RTN modeling. Fig.14 shows a possible explanation of the V_{GS} dependence of λ; trap density vs. energy may be decaying from the valence band side to conduction band side.

5. Summary

Two methods useful for comprehensive understanding of RTN are proposed: a time-lag plot and a model-based statistical parameter extraction scheme. Dependence of trap number λ on V_{GS} is caused by the modulation of τc and τe by V_{GS}. Modeling of undetectable traps is important for product reliability evaluation.

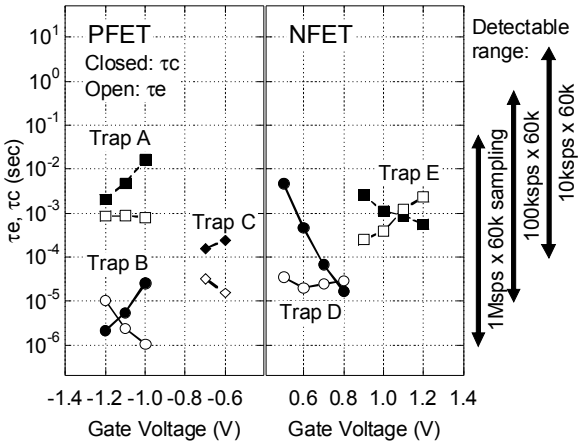

Fig. 12 Gate voltage dependence of average capture time τc and average emission time τe for some of the traps. Detectable τ ranges depending on measurement conditions are also indicated.

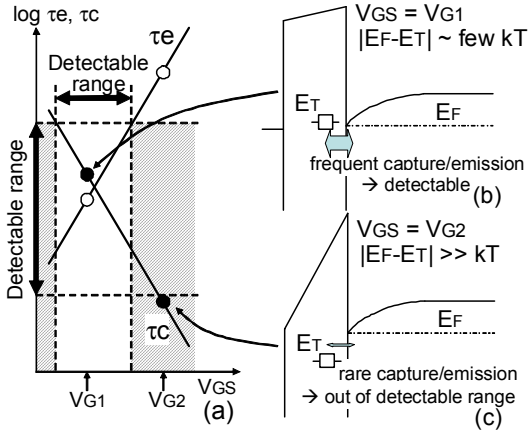

Fig. 13 (a) Schematic relationship between detectable τ range and V_{GS} range for round-trip type trap (traps B, C, E) in Fig.12. (b) Schematic band diagram at $V_{GS} = V_{G1}$. (c) Schematic band diagram at $V_{GS} = V_{G2}$.

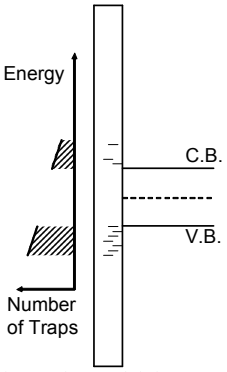

Fig. 14 One possible picture for explaining V_{GS} dependence of λ in Fig. 10. Trap density decays form valence band side to conduction band side.

References

[1] N. Tega et al., 2008 IRPS, p.541.
[2] N. Tega et al., 2009 Symp. VLSI Tech., p.50.
[3] K. Takeuchi et al., 2009 Symp. VLSI Tech., p.54.
[4] K. Abe et al., Jpn. J. Appl. Phys., v. 48, n. 4, 04C044, 2009..
[5] T. Shimizu et al., 2009 IRPS, p.389.
[6] A. Asenov et al., 2000 IEDM, p.27
[7] Z. Shi et al., IEEE Trans. Electron Devices, v. 41, n. 7, p. 1161, 1994.